Article:
De Domenico, D. and Askes, H. (2018) Nano-scale wave dispersion beyond the First Brillouin Zone simulated with inertia gradient continua. Journal of Applied Physics, 124. ISSN: 0021-8979

https://doi.org/10.1063/1.5045838

Nano-scale wave dispersion beyond the First Brillouin Zone simulated with inertia gradient continua

Dario De Domenico*
Department of Engineering, Università degli Studi di Messina, Contrado Di Dio, 98166 Sant'Agata, Messina, Italy

Harm Askes†
Department of Civil and Structural Engineering, University of Sheffield, Mappin Street, Sheffield S1 3JD, United Kingdom

Nano-scale wave dispersion beyond the First Brillouin Zone is often observed as descending branches and inflection points when plotting frequency or phase velocity against the wave number. Modelling this with discrete chain models is hampered by their restricted resolution. A continuum model equipped with higher-order inertia gradients is here developed as a suitable and versatile alternative. This model can be derived from discrete chain models, thereby providing a lower-scale motivation for the higher-order gradient terms. The derived gradient model is without free parameters, as the material constants are calculated a priori by minimising the error with respect to the discrete chain response. Unlike asymptotic approximations that provide a best fit for vanishing wave numbers, the error is here minimised over the entire range of reduced wave numbers 0 to 1, which leads to a much improved accuracy beyond the First Brillouin Zone. The new gradient model has been validated against (i) phonon dispersion curves measured through neutron scattering experiments in bismuth, aluminium and nickel, and (ii) Molecular Dynamics (MD) flexural wave propagation simulations of Carbon Nanotubes (CNTs). The model captures all qualitative aspects of the experimental and MD dispersion curves without requiring bespoke curve fitting procedure. With the exception of one set of MD results, the accuracy of the gradient model is very good.

I. INTRODUCTION

Dispersion of propagating waves occurs if the wave length is of the same order of magnitude as the characteristic spacing of the dominant source of heterogeneity. Experimental evidence exists of phonon dispersion in lattice materials[1–5], and this has been backed up by molecular dynamics simulations[6–8]. The majority of these studies focus on waves whose half wave length is larger than the lattice spacing — a cut-off point known as the First Brillouin Zone (FBZ). However, some limited experimental evidence is available for waves with shorter wave lengths, and this indicates that these very short waves are still propagating, but at much reduced angular frequencies[9–12].

To simulate dispersive wave propagation beyond the FBZ, discrete lattice models are of limited use, since their spatial resolution is set by the lattice geometry. Instead, it may be more advantageous to use continuum models. However, in order to capture wave dispersion, continuum models need to be equipped with appropriate terms that capture the lower-scale behaviour — these may take the form of higher-order spatial gradients of relevant field variables[13,14].

In this paper, we will argue the case to include higher order inertia gradients in the governing equations in order to capture the dispersive effects accurately. Material-independent model parameters are obtained from a best fit of the discrete chain response across the range of relevant wave numbers k; this is superior to the straightforward application of asymptotic expansions that provide a best fit for $k \to 0$. The model is able to replicate some experimental results from the literature with good accuracy. In particular, we consider a group of phonon dispersion curves from neutron scattering measurements for a range of materials. The model is also able to approximate Molecular Dynamics simulations of bending in Carbon Nanotubes with reasonable accuracy. The same set of material-independent model parameters is used throughout the paper, thus avoiding bespoke curve fitting and/or tuning parameters.

II. STRAIN GRADIENTS OR INERTIA GRADIENTS?

An oft-used motivation for elasticity with higher-order spatial gradients is to consider asymptotic approximations of the response of a linear chain model. The linear chain is assumed to consist of masses M connected by springs with stiffness K and length ℓ, which leads to the following equation of motion for the n^{th} mass:

$$M\ddot{u}_n = K\left(u_{n+1} - 2u_n + u_{n-1}\right) \tag{1}$$

where u_n is the displacement of the n^{th} mass and a superimposed dot denotes a derivative with respect to time t. The discrete particle displacements are replaced by a continuous function u, and Taylor series are used for the continuum displacement at the neighbouring particles. This yields

$$\ddot{u} = c_e^2\left(\frac{\partial^2 u}{\partial x^2} + \frac{1}{12}\ell^2\frac{\partial^4 u}{\partial x^4} + \frac{1}{360}\ell^4\frac{\partial^6 u}{\partial x^6} + \dots\right) \tag{2}$$

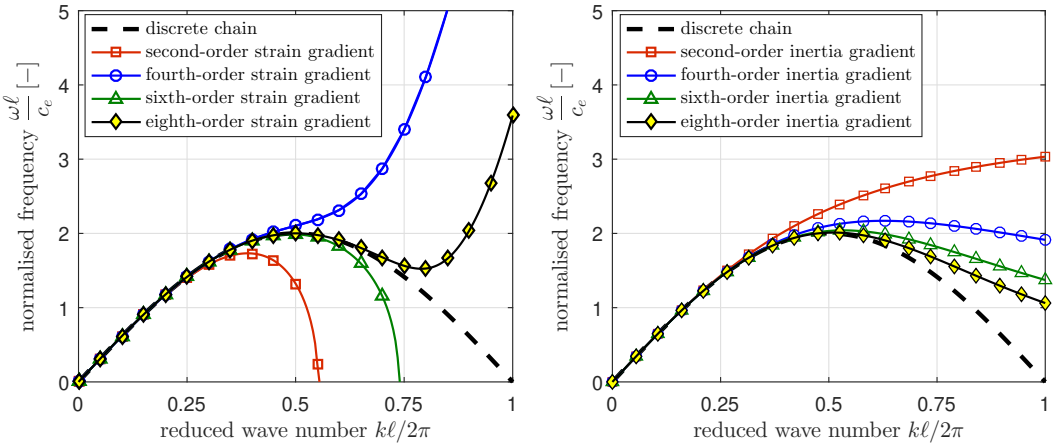

FIG. 1: Dispersion curves of discrete chain and gradient elasticity with strain gradients (left) and with inertia gradients (right)

where c_e is the elastic speed of sound. Since the higher-order terms appear on the stiffness side of the equation, the higher-order terms are called strain gradients.

As is well-known and as will be shown briefly below, models with strain gradients exhibit anomalies in dynamics. To overcome these, use can be made of asymptotic equivalence in that the strain gradients of Eq. (2) can be replaced by equivalent inertia gradients[15,16]. To do so, higher-order derivatives of Eq. (2) are taken and alternatingly substracted from or added to the original expression (2). Applying this recursively provides a $[0,n]$-Padé approximant counterpart of Eq. (2) as

$$\left(\ddot{u} - \frac{1}{12}\ell^2\frac{\partial^2\ddot{u}}{\partial x^2} + \frac{1}{240}\ell^4\frac{\partial^4\ddot{u}}{\partial x^4} - \dots\right) = c_e^2\frac{\partial^2 u}{\partial x^2} \tag{3}$$

To compare the two sets of gradient-enriched models with the original discrete model of Eq. (1), the fundamental solution $u = U\exp(\mathrm{i}(\omega t + kx))$ is substituted, where ω is the angular frequency, k is the wave number and U is the amplitude. The results for various truncations of Eqns. (2) and (3) are plotted in Figure 1. It can be seen that both sets of models show a convergence towards the discrete chain when more terms are included. However, for the strain gradient models certain truncations (second-order, sixth-order, etc.) lead to imaginary frequencies for the larger wave numbers, which in turn result in artificial model instabilities[17]. The other truncations (fourth-order, eighth-order, etc.) lead to unbounded frequencies for the larger wave numbers. Both effects are unrealistic and thus undesirable. In contrast, a monotonic convergence towards the discrete chain response is observed for the inertia gradient models, and both imaginary and unbounded angular frequencies are avoided. An inflection point is obtained for truncations of fourth-order or higher.

Whilst this shows the superiority of inertia gradients over strain gradients, the asymptotic series are expanded around $k\ell = 0$ — i.e. every truncation is a best fit for $k\ell \to 0$ rather than a best fit across the range $k\ell \in [0, 2\pi]$. As an alternative, for each individual truncation the error (in the square of the angular frequency) between discrete chain response and inertia gradient model response can be integrated over $k\ell \in [0, 2\pi]$ and then minimised with respect to the higher-order coefficients. As mentioned above, it is clear that the fourth-order term must be included if an inflection point is desired — this is the model that will be considered. The truncated model can be written generically as

$$\ddot{u} - \alpha\ell^2\frac{\partial^2\ddot{u}}{\partial x^2} + \beta\ell^4\frac{\partial^4\ddot{u}}{\partial x^4} = c_e^2\frac{\partial^2 u}{\partial x^2} \tag{4}$$

Carrying out the above error minimisation leads to

$$\alpha = \frac{6\left(32\pi^4 - 200\pi^2 + 315\right)\left(\mathrm{Si}(4\pi) - 2\mathrm{Si}(2\pi)\right)}{\pi\left(256\pi^4 - 2400\pi^2 + 4545\right)} + \frac{\frac{256}{3}\pi^5 - 600\pi^3 + 1140\pi}{\pi\left(256\pi^4 - 2400\pi^2 + 4545\right)} \tag{5a}$$

$$\beta = \frac{\left(80\pi^2 - 150\right)\left(2\mathrm{Si}(2\pi) - \mathrm{Si}(4\pi)\right) - 150\pi}{\pi\left(256\pi^4 - 2400\pi^2 + 4545\right)} \tag{5b}$$

where $\mathrm{Si}(x) = \int_0^x \sin(t)/t\mathrm{d}t$. This then leads to numerical values $\alpha \approx -0.036723$ and $\beta \approx 0.021337$.

Remark 1 *The kinetic energy density $\mathcal{K}$ underlying the model of Eq. (4) can be written as*

$$\mathcal{K} = \frac{1}{2}\left(\dot{u}^2 + \alpha\ell^2\left(\frac{\partial\dot{u}}{\partial x}\right)^2 + \beta\ell^4\left(\frac{\partial^2\dot{u}}{\partial x^2}\right)^2\right) \tag{6}$$

With the negative sign for α found in Eq. (5a), loss of positive-definiteness could lead to loss of stability. However, imaginary (and thus destabilising) frequencies can only occur for $1 + \alpha\ell^2k^2 + \beta\ell^4k^4 < 0$. For $\alpha < 0$ this would require $\beta < \frac{1}{4}\alpha^2$. It can be verified that the values reported in Eqns. (5) do not satisfy the last inequality. Thus, stability of this model is guaranteed.

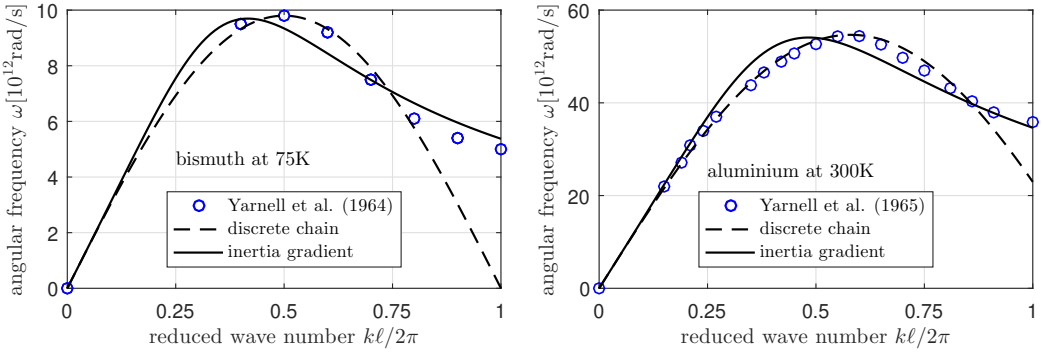

FIG. 2: Experimental results from Yarnell and coworkers for bismuth (left) and aluminium (right) simulated with discrete chain and inertia gradient models

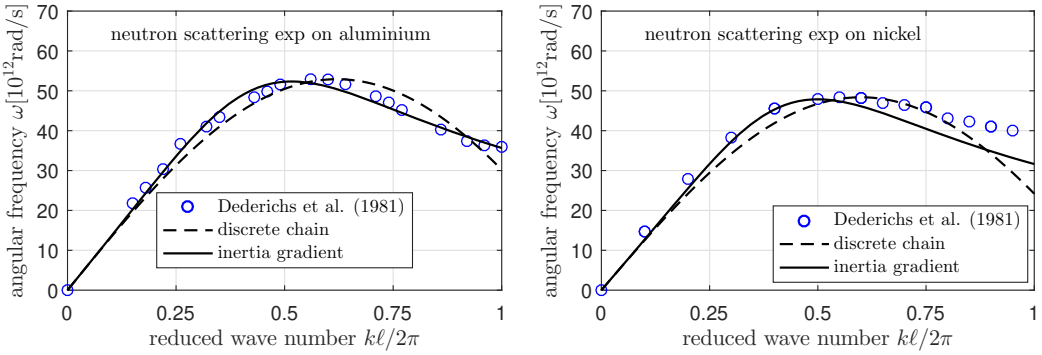

FIG. 3: Experimental results from Dederichs and coworkers for aluminium (left) and nickel (right) simulated with discrete chain and inertia gradient models

Remark 2 *A more general formulation of Eq. (4) involves a simultaneous series expansion of left-hand-side and right-hand-side, thus leading to an* $[m/n]$*-Padé approximation including strain gradients as well as inertia gradients. This allows to capture a non-zero asymptote for infinite wave numbers if required*[18,19].

III. LONGITUDINAL PHONON DISPERSION FROM NEUTRON SCATTERING MEASUREMENTS

The model of Eq. (4) with the numerical values for α β obtained above has been used to simulate the experimental results of Yarnell and coworkers from the 1960s concerning bismuth[9] and aluminium[10]. The results are shown in Figure 2, whereby the elastic constants are fitted such that the peak in the experimental results coincides with the maximum of the discrete chain response. Note that for the case of aluminium, the experimentally reported values did not have their maximum at $k\ell = \pi$; to correct this, we have adjusted the horizontal scaling of the two model responses slightly. It can be seen that the accuracy of the discrete chain model is better for the pre-peak part of the curve, but that of the inertia gradient model is better able to capture the post-peak part of the curve. Overall, the inertia gradient model captures all qualitative aspects of the experimental results.

An additional set of neutron scattering measurements of Al and Ni beyond the FBZ were reported by Dederichs et al.[11] and more recently referenced in other simulation approaches[12]. These additional phonon dispersions curves are reported in Figure 3 and compared with the corresponding predictions from discrete chain and inertia gradient models. Again it is seen that the inertia gradient model is able to capture these experimental results with good accuracy without the need to carry out additional parameter calibration.

IV. FLEXURAL WAVE DISPERSION IN CARBON NANOTUBES

Next, the efficacy of the model with inertia gradients to emulate the flexural behaviour of Carbon Nanotubes (CNTs) is verified. As has been shown in various earlier studies, it is expedient to adopt beam bending theories from structural mechanics[20–27], with in more recent years an expanding range of applications and novel solutions[28,29]. Timoshenko beam theory is particularly

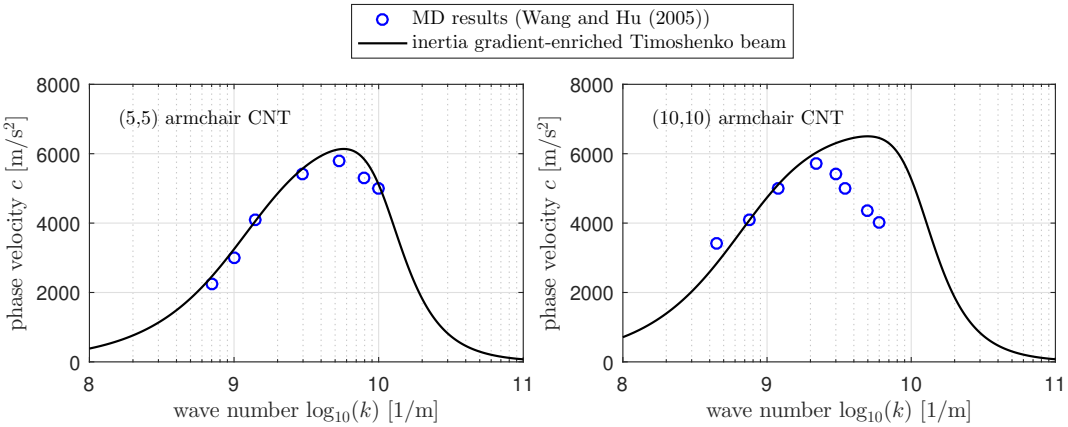

FIG. 4: MD results from Wang and Hu for a (5,5) CNT (left) and a (10,10) CNT (right) simulated with inertia gradient models

suitable for the modelling of relatively short beams, which in the context of CNTs means that this theory is appropriate for the modelling of relatively short wave lengths.

Adopting a coordinate system with the x-axis along the beam, the coupled equations of standard Timoshenko beam theory read

$$\rho A\ddot{w} = \chi GA\left(\frac{\partial^2 w}{\partial x^2} - \frac{\partial \phi}{\partial x}\right) \tag{7a}$$

$$\rho I\ddot{\phi} = \chi GA\left(\frac{\partial w}{\partial x} - \phi\right) + EI\frac{\partial^2 \phi}{\partial x^2} \tag{7b}$$

Here, E and G are the Young's modulus and shear modulus of the material, τ and σ are the transverse shear stress and axial normal stress, whilst the primary unknowns are the transverse displacement w and the rotation of the cross section ϕ. Furthermore, $A = 2\pi Rt$ and $I = \pi\left(R^3 t + \frac{1}{4}Rt^3\right)$ are the area and the second moment of area of the cross section, respectively, with R the radius and t the wall thickness of the CNT. Finally, χ is the so-called "shear correction factor" and is a dimensionless constant that depends on the geometry of the cross-section (e.g. $\chi = \frac{1}{2}$ for thin-walled cylinders).

In the spirit of Eq. (4), the inertia sides of these two equations are expanded with higher-order inertia gradients of the relevant kinematic state variable. The gradient-enriched Timoshenko theory is thus given by

$$\rho A\left(\ddot{w} - \alpha\ell^2\frac{\partial^2 \ddot{w}}{\partial x^2} + \beta\ell^4\frac{\partial^4 \ddot{w}}{\partial x^4}\right) = \chi GA\left(\frac{\partial^2 w}{\partial x^2} - \frac{\partial \phi}{\partial x}\right) \tag{8a}$$

$$\rho I\left(\ddot{\phi} - \alpha\ell^2\frac{\partial^2 \ddot{\phi}}{\partial x^2} + \beta\ell^4\frac{\partial^4 \ddot{\phi}}{\partial x^4}\right) = \chi GA\left(\frac{\partial w}{\partial x} - \phi\right) + EI\frac{\partial^2 \phi}{\partial x^2} \tag{8b}$$

Simultaneous solutions $w(x,t) = W\exp\left(\mathrm{i}k(x-ct)\right)$ and $\phi(x,t) = \Phi\exp\left(\mathrm{i}k(x-ct)\right)$ are substituted, and after elimination of the amplitudes W and Φ a quartic equation in terms of the phase velocity c is found as

$$\frac{c^4}{c_e^4}\left(1+\alpha\ell^2k^2+\beta\ell^4k^4\right) - \frac{c^2}{c_e^2}\left(\frac{\chi G}{E}+\frac{\chi GA}{EIk^2}+1\right) + \frac{\chi G}{E\left(1+\alpha\ell^2k^2+\beta\ell^4k^4\right)} = 0 \tag{9}$$

This equation has two solutions for c^2, the higher of which is the optical mode and the lower of which is the acoustic mode. The latter has been verified against the Molecular Dynamics (MD) results of Wang and Hu[20] for (5,5) and (10,10) armchair CNTs. These authors reported $\rho = 2237$ kg/m^3, with $E = 460$ GN/m^2 and Poisson's ratio $\nu = 0.22$ for the (5,5) CNT while $E = 470$ GN/m^2 and $\nu = 0.20$ for the (10,10) CNT.

With a C–C bond length $b = 0.142$ nm, the closest longitudinal distance between two rings of atoms in an armchair CNT equals $\frac{1}{2}b\sqrt{3} = 0.123$ nm. However, it must be realised that consecutive rings of atoms are offset in a circumferential sense. The correct periodicity is obtained by a translation over a distance $b\sqrt{3} = 0.246$ nm, and we propose that this is the correct analogue of longitudinal atomic spacing in an armchair CNT. Thus, we take $\ell = b\sqrt{3} = 0.246$ nm. The radius of the CNT can be found from $R = 3nb/2\pi$ where $n = 5$ or $n = 10$. Finally, for the wall-thickness we have followed the recommendations of Vodenitcharova and Zhang[30] and taken $t = 0.0617$ nm.

We have used the material-independent values of α and β obtained in Eqns. (5) to emulate the results of Wang and Hu. Thus, we are avoiding further bespoke curve fitting by assuming again the discrete model as an objective measure for calculating the model coefficients not only for longitudinal wave dispersion, but also for flexural wave propagation simulations. Figure 4 shows the results for both CNTs. The material-independent values of α and β provide a good approximation of the MD results for the

(5,5) CNT. On the other hand, for the (10,10) CNT the material-independent values of α and β lead to a much larger discrepancy between inertia gradient beam theory and MD results — in fact, a similar loss of accuracy is present in the work of Wang and Hu who used a different gradient enrichment of Timoshenko beam theory.

Remark 3 *Vodenitcharova and Zhang also argued the case for a much larger value for the Young's modulus of CNTs compared to that reported by Wang and Hu. We have not taken this larger value but instead used those reported by Wang and Hu as indicated above, since this allows us to adopt the MD results of Wang and Hu without modification of the speed of sound and, thus, the vertical scaling in Figure 4.*

V. CONCLUSIONS

In order to simulate elastic wave dispersion, continuum models equipped with higher-order inertia terms are superior to continuum models equipped with higher-order strain gradient terms. We have suggested a model with two higher-order inertia gradients which allows to capture the inflection point beyond the First Brillouin Zone observed in experiments. We have also used this continuum model to formulate a novel Timoshenko beam theory with inertia gradients in order to capture flexural wave dispersion in Carbon Nanotubes.

A material-independent best fit of the coefficients of the higher-order terms has been shown to give good approximations of longitudinal dispersive wave propagation for a range of materials. The same parameter also allows to capture flexural wave dispersion in CNTs. The accuracy of the gradient model for CNTs with a relatively small radius is good; the accuracy of the model for CNTs with a larger radius is less — the latter observation is consistent with the work of Wang and Hu who provided the Molecular Dynamics benchmark solution as well as their own Timoshenko beam theory approximation.

It is emphasized here that the model discussed in this paper is without free parameter and can, thus, be used straightforwardly without requiring any experimental calibration. This offers advantages over most other gradient models used in the literature, which typically require bespoke, material-dependent calibration from experimental data to be usable.

* Electronic address: dario.dedomenico@unime.it
† Electronic address: h.askes@sheffield.ac.uk

[1] J.L. Warren, J.L. Yarnell, G. Dolling and R.A. Cowley, Phys. Rev. **158**, pp. 805–808 (1967).
[2] J.L. Verble, J.L. Warren and J.L. Yarnell, Phys. Rev. **168**, pp. 980–989 (1968).
[3] G.N. Savin and A.A. Lukashev and E.M. Lysko, Int. Appl. Mech. **6**, pp. 725–728 (1970).
[4] D.L. Price and J.M. Rowe and R.M. Nicklow, Phys. Rev. B **3**, pp. 1268–1279 (1971).
[5] K. Jakata and A.G. Every, Phys. Rev. B **77**, 174301 (2008).
[6] A.H. Opie and J. Grindlay, J. Phys. C **5**, pp. 3289–3295 (1972).
[7] D.P. DiVincenzo, Phys. Rev. B **34**, pp. 5450–5465 (1986).
[8] R. Maranganti and P. Sharma, J. Mech. Phys. Sol. **55**, pp. 1823–1852 (2007).
[9] J.L. Yarnell, J.L. Warren, R.G. Wenzel and S.H. Koenig, IBM Journal **8**, pp. 234–240 (1964).
[10] J.L. Yarnell, J.L. Warren and S.H. Koenig, in *Lattice Dynamics*, ed. R.F. Wallis, pp. 57–61 (1965).
[11] P.H. Dederichs, H. Schober, and D.J. Sellmyer, Phonon states of elements. Electron states and fermi surfaces of alloys. Berlin, Heidelberg: Springer, (1981).
[12] Y. Wang, Z.K. Liu, and L.Q. Chen, Acta Materialia **52**(9), pp. 2665-2671 (2004).
[13] H. Askes and E.C. Aifantis, Int. J. Sol. Struct. **48**, pp. 1962–1990 (2011).
[14] E.C. Aifantis, Adv. Appl. Mech. **49**, pp. 1-110 (2016).
[15] M.B. Rubin, P. Rosenau and O. Gottlieb, J. Appl. Phys. **77**, pp. 4054–4063 (1995).
[16] I.V. Andrianov and J. Awrejcewicz and R.G. Barantsev, ASME Appl. Mech. Rev. **56**, pp. 87–110 (2003).
[17] T.M. Michelitsch, I.M. Gitman and H. Askes, Mech. Res. Comm. **34**, pp. 515–521 (2007).
[18] D. De Domenico and H. Askes, Int. J. Numer. Meth. Engng **108**, pp. 485–512 (2016).
[19] D. De Domenico, H. Askes, Int. J. Numer. Meth. Engng **109**, pp. 52-72 (2017).
[20] L. Wang and H. Hu, Phys. Rev. B **71**, 195412 (2005).
[21] Q. Wang, J. Appl. Phys. **98**, 124301 (2005).
[22] C.M. Wang, Y.Y. Zhang and X.Q. He, Nanotechn. **18**, 105401 (2007).
[23] Q. Wang and C.M. Wang, Nanotechn. **18**, 075702 (2007).
[24] W.H. Duan, C.M. Wang and Y.Y. Zhang, J. Appl. Phys. **101**, 024305 (2007).
[25] C.W. Lim and C.M. Wang, J. Appl. Phys. **101**, 054312 (2007).
[26] J.N. Reddy and S.D. Pang, J. Appl. Phys. **103**, 023511 (2008).
[27] H. Askes and E.C. Aifantis, Phys. Rev. B **80**, 195412 (2009).
[28] M.A. Eltaher, M.E. Khater and S.A. Emam, Appl. Math. Modelling **40**, pp. 4109–4128 (2016).
[29] H. Rafii-Tabar, E. Ghavanloo and S.A. Fazelzadeh, Phys. Reports **638**, pp. 1-97 (2016).
[30] T. Vodenitcharova and L.C. Zhang, Phys. Rev. B **68**, 165401 (2003).